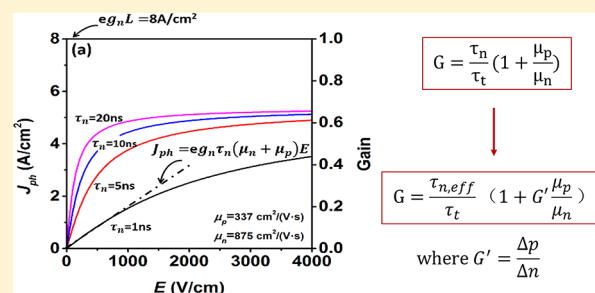# A Photoconductor Intrinsically Has No Gain

Yaping Dan,*,[†] Xingyan Zhao,[†] Kaixiang Chen,[†] and Abdelmadjid Mesli[‡]

[†]University of Michigan−Shanghai Jiao Tong University Joint Institute, Shanghai Jiao Tong University, 800 Dong Chuan Road, Shanghai, China

[‡]Institute Matériaux Microélectronique Nanosciences de Provence, UMR 6242 CNRS, Université Aix-Marseille, 13397 Marseille, Cedex 20, France

S *Supporting Information*

ABSTRACT: In the past 50 years, the high gain in quantum efficiency of photoconductors is often explained by a widely accepted theory in which the photogain is proportional to the minority carrier lifetime and inversely proportional to the carrier transit time across the photoconductor. It occasionally misleads scientists to believe that a high-speed and high-gain photodetector can be made simply by shortening the device length. The theory is derived on the assumption that the distribution of photogenerated excess carriers is spatially uniform. In this Letter, we find that this assumption is not valid for a photoconductive semiconductor due to the metal−semiconductor boundary at the two metal electrodes inducing carrier confinement. By solving the continuity equation and performing numerical simulations, we conclude that a photoconductor intrinsically has no gain or at least no high gain, no matter how short the transit time and how long the minority lifetime is. The high gain observed in experiments comes from other extrinsic effects such as defects, surface states, and surface depletion regions that localize excess minority carriers, leaving a large number of excess majority carriers accumulated in the conduction channel for the photogain. Following the Ohm's Law, a universal equation governing the photogain in a photoconductor is established at the end of this Letter.

KEYWORDS: *photoconductor, photogain mechanism, minority carrier lifetime, transit time, carrier recycling, trap states*

$eg_nL = 8 A/cm^2$

$J_{ph} = eg_n\tau_n(\mu_n + \mu_p)E$

$\tau_n = 20ns$
$\tau_n = 10ns$
$\tau_n = 5ns$
$\tau_n = 1ns$

$\mu_p = 337\ cm^2/(V\cdot s)$
$\mu_n = 875\ cm^2/(V\cdot s)$

$$G = \frac{\tau_n}{\tau_t}\left(1 + \frac{\mu_p}{\mu_n}\right)$$

$$G = \frac{\tau_{n,eff}}{\tau_t}\left(1 + G'\frac{\mu_p}{\mu_n}\right)$$

where $G' = \frac{\Delta p}{\Delta n}$

It is well-known that avalanche photodiodes and bipolar phototransistors have gain in terms of quantum efficiency. A photoconductive semiconductor having gain is surprising, but it is clearly written in the classical semiconductor physics textbooks[1−3] and widely accepted by the research community for decades.[4−8] The gain theory was derived in the 1950s,[9] which concluded that the gain of a photoconductor is equal to the recombination lifetime of minority carriers divided by the transit time that the carriers take to transport across the semiconductor between the two contacts of the device. Therefore, a photoconductor will intrinsically have a large gain if the transit time is much shorter than the recombination lifetime. The physical explanation for the gain is that the short transit time allows the photogenerated carriers to circulate in the circuit multiple times before recombination, equivalent to generating many times more photoexcited carriers.[1] We call this gain theory as "recycling gain mechanism" for convenience.

Conceptually, according to the theory, the recycling of charge carriers increases the number of collected carriers but not the concentration of excess carriers in the device. The theory will inevitably lead to the conclusion of no gain in photoconductivity, which however is in contradiction with most of the experimental observations.[4,8] Quantitatively, there is a huge disparity between the gains predicted by the theory and those measured in experiments. For instance, Matsuo et al.[10] observed in 1984 that the gain of GaAs photoconductive detectors predicted by the recycling gain theory is 3−4 orders of magnitude smaller than the gain measured in the experiments. Similar observations have been made persistently by other researchers in the past several decades.[4,11,12] Some argued that this disparity is due to the carrier trapping by surface trap states or charge separation by built-in electric fields that increases the recombination lifetime of minority carriers.[6,13,14] Others even mixed up the concepts of trap-emission and minority recombination lifetimes,[4] using the long trap lifetime to replace the short minority recombination lifetime to explain away the disparity. Up to date, this gain theory is still being widely used to explain the observed photoconductive gain in photoconductors based on quantum dots,[15] nanowires[7,16] and more recently 2-dimensional materials.[17,18]

In this Letter, we find that this well-known recycling gain theory is highly questionable because its derivation does not consider the metal−semiconductor boundary and is based on the assumption that the concentration of photogenerated excess carriers in the photoconductor is uniformly distributed. However, for a semiconductor in contact with metal (as
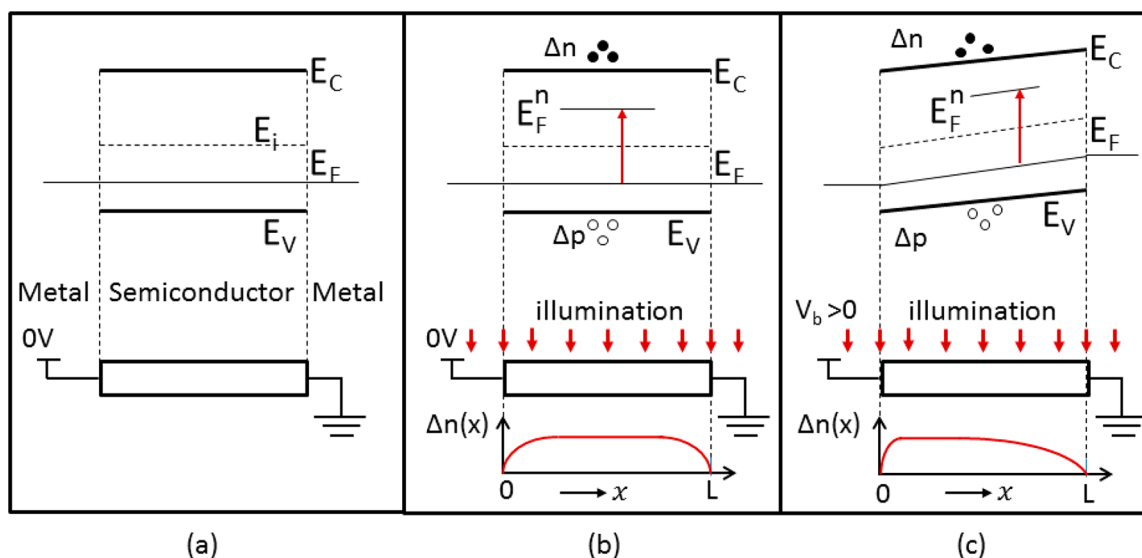
Figure 1. Energy band diagram of a photoconductor (a) in the dark, (b) under light illumination with zero voltage bias, and (c) under light illumination with nonzero voltage bias. The semiconductor is assumed to have the same work function with the metal.

electrodes), the photogenerated excess carriers in the semiconductor are always spatially nonuniform due to the carrier confinement by the metal−semiconductor boundary and, therefore, electric-field dependent. By solving the continuity equation and performing simulations using the commercial device simulator, we conclude that a photoconductor intrinsically has no gain or at least no high gain. It means that, for a photoconductive semiconductor in contact with metal electrodes, the theoretical gain will never be greater than 1 or at most not greater than the ratio of the majority to minority mobility, no matter how short the transit time and how long the minority lifetime is. In the latter case, it might be higher than 1 if the majority carrier mobility is larger than the minority carrier mobility. The high gain observed in experiments comes from other extrinsic effects such as the trapping effect of defects, surface states, and surface depletion regions that will localize excess minority carriers and leave a large number of excess majority counterparts accumulated in the conduction channel, leading thus to the observed high photogain. Following the Ohm's Law, a new equation governing the photogain in photoconductors is established at the end of this Letter.

Let us first go through the theoretical derivation of the recycling gain mechanism in the classical semiconductor physics textbooks.[1] The gain G of a photoconductor following the definition of internal quantum efficiency is defined as the number of photogenerated charge carriers collected by the electrodes divided by the number of photons absorbed in the semiconducting photoconductor.

$$G = \frac{N_{electron}}{N_{photon}} = \frac{J_{ph} \cdot A_c/e}{P_{abs}/\hbar\omega} \tag{1}$$

where J_{ph} is the photocurrent density, A_c the cross-sectional area of the device, e the charge unit, and $\hbar\omega$ the photon energy. The denominator $P_{abs}/\hbar\omega$ is the total number of photons absorbed per second in the device. If we assume one absorbed photon generating one electron−hole pair, the carrier generation rate is equal to $g = P_{abs}/\hbar\omega/V$, where V is the device volume given by $V = A_c \times L$, with L being the length

between the two electrodes of the photoconductor. Then eq 1 can be further written as eq 2:

$$G = \frac{N_{electron}}{N_{photon}} = \frac{J_{ph} \cdot A_c/e}{P_{abs}/\hbar\omega} = \frac{J_{ph}}{egL} \tag{2}$$

The photocurrent density equals to $J_{ph} = e(\mu_n\Delta n + \mu_p\Delta p)\cdot E$, in which E is the electric field intensity, μ_n and μ_p are the electron and hole mobility, and Δn and Δp are the photogenerated electron and hole concentration, respectively, and $\Delta n = \Delta p$ as the excess carriers are generated in pairs. In general, the photogenerated minority carrier concentration can be written as eq 3:

$$\Delta n = g\cdot\tau_n \tag{3}$$

where g is the generation rate and τ_n is the recombination lifetime of minority electrons in a semiconductor. Note that τ_n is determined by the quality of the semiconductor at the atomic level. The incorporation of a given amount of defects and impurities is unavoidable.

By plugging eq 3 into eq 2, we get the following:

$$G = \frac{\tau_n(\mu_n + \mu_p)E}{L} = \frac{\tau_n}{\tau_t}\left(1 + \frac{\mu_p}{\mu_n}\right) \tag{4}$$

in which $\tau_t = L/(\mu_n E)$ is the transit time for the minority electrons to transport between the two contact electrodes of the photoconductor. Note that the transit time has a low limit due to the velocity saturation. Nevertheless, the gain according to eq 4 can still be very high if the recombination lifetime is much longer than the transit time by applying a large electric voltage on a short device.

Equation 4 is the theoretical foundation of the recycling gain mechanism. The main problem of this theory originates from eq 3, which is assumed to be spatially uniform and independent of the electric field intensity. But for a semiconductor in contact with metal, the distribution of photogenerated excess carriers is always nonuniform and therefore readily skewed by the electric field, resulting in the voltage-dependent excess carrier concentration. This can be seen clearly from the continuity equation. For a uniformly

doped p-type semiconductor under small injection condition, the continuity equation at steady state for minority carriers is expressed as

$$D_n \frac{\partial^2 \Delta n}{\partial x^2} + \mu_n E \frac{\partial \Delta n}{\partial x} + \mu_n \Delta n \frac{\partial E}{\partial x} - \frac{\Delta n}{\tau_n} + g_n = 0 \quad (5)$$

where D_n, μ_n, τ_n, and g_n are the diffusion constant, mobility, recombination lifetime, and generation rate of minority electrons, respectively. With voltage bias, the electric field inside the device may be uniform (Ohmic contact) but always nonzero. The uniform electric field will zero out the third term. On the other hand, the second and consequently the first term are zero, only if the excess carriers are uniformly distributed. In this case, eq 3 is valid.

However, the distribution of photogenerated excess carrier in a semiconductor in contact with metal is always nonuniform, as shown in Figure 1. For simplicity, we assume that the semiconductor is in Ohmic contacts with the metal electrodes by having the same work function with the metal. (Other types of Ohmic contacts formed by silicides or tunneling Schottky barriers are also studied. See SI, Section 1. The results are consistent with what we find below.) There is no energy band bending when they are in contact (Figure 1a). Light is uniformly illuminated on the device from the vertical direction, as shown in the sketch of Figure 1b. Excess minority electrons are excited in the conduction band in the semiconductor and no excess electrons will be generated in the metal. To maintain continuity, the concentration of excess minority electrons has to be zero at the semiconductor−metal interface, resulting in excess electrons in the semiconductor diffusing toward the metal, as shown in the bottom sketch of Figure 1b. At zero voltage bias, the electron diffusion is antisymmetric with no net photocurrent flow in the circuit. At nonzero bias, the electric field will skew the antisymmetric transport of excess electrons (Figure 1c), creating a net photocurrent. Clearly, the concentration of photogenerated excess carriers is spatially voltage-dependent instead of following the simple expression of eq 3. If eq 3 cannot hold, then the gain expression eq 4 derived on the basis of eq 3 is questionable.

To derive the correct expression for the gain, we need to first find the minority carrier distribution by solving the continuity eq 5 with the assumption of uniform electric field (the third term is zero). This assumption is valid for a uniformly doped semiconductor with Ohmic contact at small injection condition. By applying the boundary conditions $\Delta n = 0$ at both $x = 0$ and $x = L$, we find

$$\Delta n(x) = g_n \tau_n \frac{1 - \exp(\lambda_2 L)}{\exp(\lambda_2 L) - \exp(\lambda_1 L)} \cdot \exp(\lambda_1 x)$$
$$- g_n \tau_n \frac{1 - \exp(\lambda_1 L)}{\exp(\lambda_2 L) - \exp(\lambda_1 L)} \cdot \exp(\lambda_2 x) + g_n \tau_n \quad (6)$$

where $\lambda_{1,2} = \frac{-L_{dr}(E) \pm \sqrt{L_{dr}^2(E) + 4L_D^2}}{2L_D^2}$ ("+" for λ_1 and "−" for λ_2) with the drift length $L_{dr} = \mu_n \tau_n E$ and the diffusion length $L_D = \sqrt{D_n \tau_n}$.

To validate the solution of the continuity equation given by eq 6, we performed numerical simulations on a silicon photoconductor using the DEVICE module of the commercial software Lumerical. The software module numerically solves the Poisson's equation and the continuity equations for minority and majority carriers. It can catch the transport behavior of both types of carriers, providing more realistic

results. We suppose that the device under simulation is 50 μm long and 1 μm × 1 μm in cross-section. The p-type doping concentration is 10^{17} cm^{-3} and the generation rate is spatially uniform at 10^{22} cm^{-3}/s for the sake of clarity. The recombination lifetime of minority carriers is set at 1 ns due to, for instance, defects and impurities as recombination centers. The mobility for electrons and holes is 875 cm^2/(V s) and 337 cm^2/(V s), respectively. Different lifetime and mobility for electrons and holes will not change the conclusion (see more discussions later). As we show later, the photocurrent will saturate at high voltage bias. To illustrate that the photocurrent saturation is not caused by the velocity saturation, the velocity saturation effect is excluded from the simulation. The spatial distributions of photogenerated excess carriers are plotted in Figure 2. The solid and dotted lines
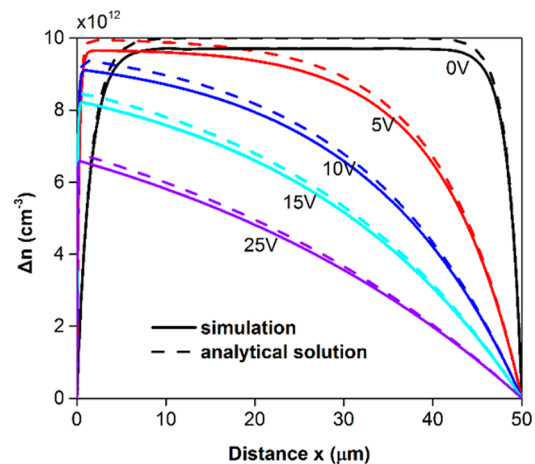
Figure 2. Spatial distribution of photogenerated excess minority carriers in a photoconductor. Dotted lines are the solutions of the continuity equation and solid lines are the simulation results. Velocity saturation is excluded from the simulation.

denote the concentrations of excess minority carriers Δn given by the device simulator and eq 6, respectively. It is clear that the simulation results and the solutions of the continuity equation are almost identical.

$$J_n = -e D_n g_n \tau_n \frac{\lambda_2 (1 - e^{\lambda_1 L})(1 + e^{\lambda_2 L}) - \lambda_1 (1 - e^{\lambda_2 L})(1 + e^{\lambda_1 L})}{e^{\lambda_2 L} - e^{\lambda_1 L}}$$
$$= \begin{cases} e g_n \tau_n \mu_n E & E \to 0, L_D \ll L \\ e g_n L & E \to \infty \end{cases} \quad (7)$$

As expected, the antisymmetric distribution of the excess carriers is skewed by the electric field (Figure 2), which will create net photocurrent in the circuit. The equation for the minority photocurrent is given by eq 7. This expression is rather complicated but it can be simplified to the forms that we are more familiar with at two extreme cases. The first case is when the electric field intensity is close to zero. The drift length (L_{dr}) is then nearly zero, much smaller than the diffusion length (L_D). Logically, the transit time of minority carriers will be significantly longer than the recombination lifetime, that is, $\tau_n/\tau_t \ll 1$. In this case, the spatial distribution of photogenerated excess minority carriers remains almost antisymmetric. If the diffusion length L_D is much smaller than the device length L, then the excess minority carriers distribute almost uniformly in the semiconductor. The uniform distribution of photogenerated carriers and electric field will
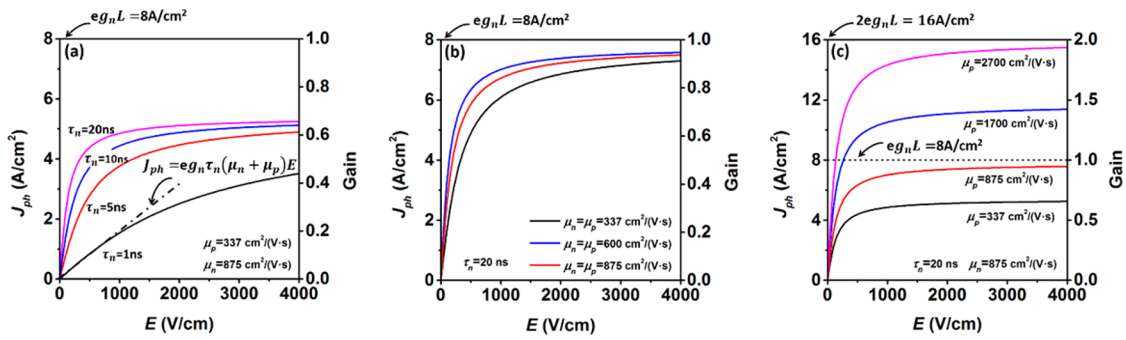
Figure 3. Photocurrent density vs electric field intensity. The device has the same parameters with the one in Figure 2 except for the minority recombination lifetime and mobility. (a) Photocurrent saturates to a value smaller than egL if the majority carrier mobility is smaller than the minority carrier mobility. A longer minority carrier lifetime will not make the photocurrent saturate to a higher value but saturate faster. (b) Photocurrent saturates to egL when the electron and hole mobility are equal. (c) Photocurrent saturates to a value larger than egL when the majority mobility is bigger than the minority mobility.

zero out the first three terms in eq 5, resulting in $\Delta n = g_n\tau_n$. The photocurrent density of minority excess carriers will then be given by $J_n = eg_n\tau_n\mu_n E$, consistent with the simplification in eq 7 for a small electric field. For the case that the electric field intensity E approaches very large values, the excess carrier distribution is strongly skewed (like the curve at 25 V bias in Figure 2). The equation $\Delta n = g_n\tau_n$ will never satisfy. In this case, the transit time will be much shorter than the recombination lifetime, that is, $\tau_n/\tau_t \gg 1$. The minority electron photocurrent density saturates to $J_n = eg_nL$ instead of linearly going up, as shown in eq 7. This is not surprising if we take into account the fact that the concentration of excess minority carriers decreases as the bias increases, as shown in Figure 2.

The photogenerated excess majority carriers Δp also contribute to the photocurrent. Note that the semiconductor is doped. There is a large background dark current contributed by the majority carriers. The continuity equation for majority carriers is a nonlinear differential equation, from which it is difficult to analytically solve the spatial distribution of the excess majority carriers. Nevertheless, it is known (we also verified by simulations, see SI, section 2) that the spatial distributions of excess majority and minority carriers are nearly identical if the external electric field is not too high, regardless of the difference in mobility for minority and majority carriers. This phenomenon is called ambipolar transport.[1] As stated above, the excess minority electrons $\Delta n = g_n\tau_n$ are mostly uniformly distributed and the electron photocurrent density is given by $J_n = eg_n\tau_n\mu_n E$ on the condition that the electric field intensity E is not strong and the diffusion length is much smaller than the device length L (Figure 1b). Due to the ambipolar transport phenomenon, the same conclusion can be reached for the excess majority holes, i.e. $\Delta p = g_n\tau_n$ and $J_p = eg_n\tau_n\mu_p E$. Therefore, the total photocurrent density is governed by $J_{ph} = eg_n\tau_n(\mu_n + \mu_p)E$, which is consistent with the common knowledge and the simulation results shown in Figure 3a at small voltages. In this case, the gain expression given by eq 4 still holds except that the gain is much smaller than 1, because $\tau_n/\tau_t \ll 1$ at small electric field intensity as previously analyzed for the minority carriers.

At high electric field, the total photocurrent density, instead of increasing linearly, saturates to a value that is only a fraction of $J_{ph} = eg_nL$ (gain less than 1, see eq 2), although the excess electron current approaches $J_n = eg_nL$ (eq 6). This is because the slower excess majority holes will accumulate in the

semiconductor (the majority hole mobility is smaller than the minority electron mobility in Figure 3a), inducing a small built-in electric field that partially cancels out the electron photocurrent. A longer minority lifetime does not increase the total photocurrent. Instead, it will only make the photocurrent saturate at smaller electric field (Figure 3a). If the majority and minority excess carriers have the same mobility, the built-in electric field disappears and the total current saturates at $J_n = eg_nL$ (Figure 3b with gain approaching but never exceeding 1). If the majority carriers have a higher mobility than the minority carriers (Figure 3c), the saturation photocurrent becomes higher than $J_{ph} = eg_nL$, creating some photogain in the device. As the majority carrier mobility continues to increase, this photogain becomes even higher (Figure 3c), but not higher than the ratio of the majority to minority mobility. Clearly, this small gain cannot explain the widely observed high photo gains in literature. We can therefore conclude that a photoconductor intrinsically has no gain, or at least no high gain, no matter how short the transit time and how long the minority lifetime is.

If a photoconductor intrinsically has no gain or no high gain, then where are the high gains observed in the experiments coming from?

We recently revealed by photo Hall effect measurements[19] that a silicon nanowire with a high photogain always has an unusually high concentration of excess majority carriers compared to minority excess carriers, that is, $\Delta p \gg \Delta n$ (assume holes as majority carriers). This experimental observation indicates that the assumption of an equal concentration for excess minority and majority carriers ($\Delta p = \Delta n$) may not always be valid during the derivation of eq 4. To make it more general, we relax this constraint by defining $G' = \Delta p/\Delta n$ as a gain in excess carrier concentration so that eq 4 can be rewritten as eq 8. If G' is large enough, G will be greater than 1 even at small bias voltage.

$$G = \frac{N_{electron}}{N_{photon}} = \frac{J_{ph}}{egL} = \frac{\tau_n}{\tau_t}\left(1 + G'\frac{\mu_p}{\mu_n}\right) \quad (8)$$

Now, the question is how it is possible to have excess majority carriers orders of magnitude higher than excess minorities in a photoconductor, since electrons and holes are generated in pairs by light illumination. Indeed, the total number of excess electrons and holes in the photoconductor are always the same. But the excess electrons and holes that contribute to the
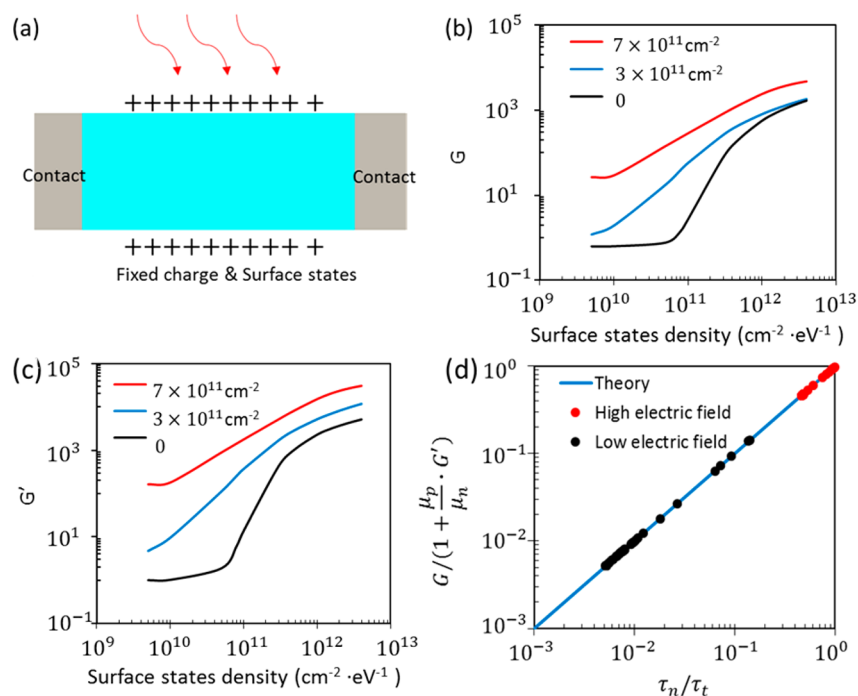
Figure 4. Photogain in the presence of fixed charges and surfaces states on the device surfaces. The silicon slab is 400 nm thick and p-type with a doping concentration of 1.05×10^{17} cm^{-3}. Device schematic is shown in (a). Photogain G in quantum efficiency (b) and gain G' in excess carrier concentration (c) are dependent on surface states density (see SI) and fixed charge concentration of 0, 3×10^{11} cm^{-2}, and 7×10^{11} cm^{-2}. eq 8 is validated by simulations in (d).

photoconductivity may not necessarily be the same, because one type of excess carriers (often minorities) may become localized via the trapping effect of defects, surface states, and surface depletion region.[20,21] The same number of the other type of counterparts (often majority carriers) is then left in the conductance channel, resulting in an unusually high G' and photogain G.

To verify this hypothesis, we performed numerical simulations on a 400 nm thick and 9 μm long silicon slab using the commercial device simulator Silvaco, as shown in Figure 4a. The light is launched perpendicularly from the top and a uniform generation g is assumed in the whole slab. We tuned the concentration of fixed charges and surface states on the top and bottom surface (see SI, section 3). The photogain G in quantum efficiency and G' in terms of gain in excess carrier concentration are plotted in Figure 4b, respectively. The photogain G is calculated according to eq 2. To plot $G' = \Delta p / \Delta n$, we need to find Δp and Δn in the photoconductor. Due to the confinement at metal−semiconductor contacts and the impact of surface fixed charges and surface states, the spatial distribution of excess electrons and holes are highly nonuniform in the conduction channel, in particular, when the concentration of fixed charges and surface states is high, resulting in a rather large photogain. It is more appropriate to use the average excess carrier concentration $\overline{\Delta p}$ and $\overline{\Delta n}$ to replace Δp and Δn, respectively. In this case, the effective minority carrier lifetime $\tau_{n,\text{eff}}$ can be written as $\tau_{n,\text{eff}} = \overline{\Delta n}/g$, where g is the carrier generation rate. When plotting $G/(1 + G'\mu_p/\mu_n)$ versus $\tau_{n,\text{eff}}/\tau_t$, with τ_t being the transit time (Figure 4c), we find that the two terms are equal to each other in a wide range of variation (all data points in Figure 4b,c), meaning that the correct equation for the photoconductor gain G shall be written as

$$G = \frac{\tau_{n,\text{eff}}}{\tau_t}\left(1 + G'\frac{\mu_p}{\mu_n}\right) \tag{9}$$

Note that $\tau_{n,\text{eff}}$ is not a constant. It depends on many parameters including intrinsic minority carrier lifetime, bias voltage, and the density of surface states. If we assume G' equals to 1, the above equation can fit perfectly the nonlinear curves in Figure 3, in which the gain can be found by normalizing the photocurrent density respective to egL (see SI, section 4). It means that the photoconductor will have no gain or at least not a high gain if there is no gain in excess carrier concentration. It is worth pointing out that eq 9 is actually universal, simply because the photocurrent density equation $J_{\text{ph}} = e(\Delta n \cdot \mu_n + \Delta p \cdot \mu_p)E$ is the Ohm's Law and no further assumption is made in the derivation. The classical gain theory contains two mistakes. First, it assumes that the concentration of excess minority carriers is spatially uniform as $\Delta n = g \cdot \tau_n$, which is only true without boundary confinement. Second, it assumes that the excess electrons and holes in the conduction channel are equal in concentration as $\Delta p = \Delta n$, which is only valid in a "perfect" semiconductor.

In conclusion, the classical gain theory is derived on the severe assumptions that boundary confinements are inexistent, leading to the wrong conclusion that a photoconductor exhibits a high gain when the minority carrier lifetime is long and the carrier transit time is short. This gain theory often misled scientists to believe that high gain and high speed photodetectors can be constructed simply by shortening the device length to minimize the transit time.[17] We prove in this work that a semiconducting photoconductor intrinsically has no gain or at least no high gain in terms of internal quantum efficiency no matter how long the minority carrier lifetime and how short the transit time is. The high photogain observed in experiments originates from a gain in the concentration of

excess charge carriers, which is induced by the trapping effect of defects, surface states, and surface depletion region. Following the Ohm's Law, we derived a universal gain equation for photoconductors, which may guide scientists to design high-performance photodetectors.

■ ASSOCIATED CONTENT

Ⓢ Supporting Information

The Supporting Information is available free of charge on the ACS Publications website at DOI: 10.1021/acsphotonics.8b00805.

Additional details and supporting figures (PDF).

■ AUTHOR INFORMATION

Corresponding Author
*E-mail: yaping.dan@sjtu.edu.cn.

ORCID Ⓞ
Yaping Dan: 0000-0002-2983-7213

Author Contributions
Y.D. conceived the concept, derived the theory, and wrote the manuscript. X.Z. performed the device simulations of Figures 1−3. K.C. performed the simulations in Figure 4. A.M. commented on the manuscript. All authors reviewed the manuscript.

Notes
The authors declare no competing financial interest.

■ ACKNOWLEDGMENTS

■ REFERENCES

(1) Neamen, D. A. *Semiconductor Physics and Devices: Basic Principles*, 4th ed.; Publishing House of Electronics Industry, 2011; Vol. *634*, p 634.

(2) Liu, E. K.; Zhu, B. S.; Luo, J. S. *Semiconductor Physics (in Chinese)*, 7th ed.; Publishing House of Electronics Industry, 2000; p 328.

(3) Sze, S. M.; Kwok, K. N. *Physics of Semiconductor Devices*, 3rd ed.; John Wiley & Sons, Inc, 2006.

(4) Konstantatos, G.; Badioli, M.; Gaudreau, L.; Osmond, J.; Bernechea, M.; de Arquer, F. P. G.; et al. Hybrid graphene-quantum dot phototransistors with ultrahigh gain. *Nat. Nanotechnol.* **2012**, *7*, 363−368.

(5) Liu, C. H.; Chang, Y. C.; Norris, T. B.; Zhong, Z. H. Graphene photodetectors with ultra-broadband and high responsivity at room temperature. *Nat. Nanotechnol.* **2014**, *9*, 273−278.

(6) Soci, C.; Zhang, A.; Bao, X. Y.; Kim, H.; Lo, Y.; Wang, D. L. Nanowire photodetectors. *J. Nanosci. Nanotechnol.* **2010**, *10*, 1430−1449.

(7) Wang, Z. X.; Safdar, M.; Jiang, C.; He, J. High-Performance UV-Visible-NIR Broad Spectral Photodetectors Based on One-Dimensional In$_2$Te$_3$ Nanostructures. *Nano Lett.* **2012**, *12*, 4715−4721.

(8) Zhang, A.; Kim, H.; Cheng, J.; Lo, Y. H. Ultrahigh Responsivity Visible and Infrared Detection Using Silicon Nanowire Photo-transistors. *Nano Lett.* **2010**, *10*, 2117−2120.

(9) Petritz, R. L. Theory of photoconductivity in semiconductor films. *Phys. Rev.* **1956**, *104*, 1508−1516.

(10) Matsuo, N.; Ohno, H.; Hasegawa, H. Mechanism of high gain in GaAs photoconductive detectors under low excitation. *Japanese Journal of Applied Physics, Part 2 (Letters)* **1984**, *23*, L299−L301.

(11) Munoz, E.; Monroy, E.; Garrido, J. A.; Izpura, I.; Sanchez, F. J.; SanchezGarcia, M. A.; et al. Photoconductor gain mechanisms in GaN ultraviolet detectors. *Appl. Phys. Lett.* **1997**, *71*, 870−872.

(12) Soci, C.; Zhang, A.; Xiang, B.; Dayeh, S. A.; Aplin, D. P. R.; Park, J.; et al. ZnO nanowire UV photodetectors with high internal gain. *Nano Lett.* **2007**, *7*, 1003−1009.

(13) Logeeswaran, V. J.; Oh, J.; Nayak, A. P.; Katzenmeyer, A. M.; Gilchrist, K. H.; Grego, S.; et al. A Perspective on Nanowire Photodetectors: Current Status, Future Challenges, and Opportunities. *IEEE J. Sel. Top. Quantum Electron.* **2011**, *17*, 1002−1032.

(14) Zardas, G. E.; Aidinis, C. J.; Anagnostakis, E. A.; Symeonides, C. I. On a predictive scheme of slow photoconductive gain evolution in expitaxial layer/substrate optoelectronic nanodevices. *Open J. Microphys.* **2011**, *1*, 32−34.

(15) Konstantatos, G.; Howard, I.; Fischer, A.; Hoogland, S.; Clifford, J.; Klem, E.; et al. Ultrasensitive solution-cast quantum dot photodetectors. *Nature* **2006**, *442*, 180−183.

(16) Jie, J. S.; Zhang, W. J.; Jiang, Y.; Meng, X. M.; Li, Y. Q.; Lee, S. T. Photoconductive characteristics of single-crystal CdS nanoribbons. *Nano Lett.* **2006**, *6*, 1887−1892.

(17) Lopez-Sanchez, O.; Lembke, D.; Kayci, M.; Radenovic, A.; Kis, A. Ultrasensitive photodetectors based on monolayer MoS$_2$. *Nat. Nanotechnol.* **2013**, *8*, 497−501.

(18) Yin, Z. Y.; Li, H.; Jiang, L.; Shi, Y. M.; Sun, Y. H.; Lu, G.; et al. Single-layer MoS$_2$ phototransistors. *ACS Nano* **2012**, *6*, 74−80.

(19) Chen, K.; He, J.; Zhao, X.; Mesli, A.; He, Y.; Dan, Y. Dynamics of charge carriers in silicon nanowire photoconductors revealed by photo Hall effect measurements. *ACS Nano* **2018**, *12*, 3436.

(20) Dan, Y. Optoelectronically probing the density of nanowire surface trap states to the single state limit. *Appl. Phys. Lett.* **2015**, *106*, 053117.

(21) Furchi, M. M.; Polyushkin, D. K.; Pospischil, A.; Mueller, T. Mechanisms of photoconductivity in atomically thin MoS$_2$. *Nano Lett.* **2014**, *14*, 6165−6170.

A photoconductor intrinsically has no gain

(Supplementary Information)

Yaping Dan[1]*, Xingyan Zhao[1], Kaixiang Chen[1] and Abdelmadjid Mesli[2]

[1]University of Michigan – Shanghai Jiao Tong University Joint Institute, Shanghai Jiao Tong University, 800 Dong Chuan Road, Shanghai, China

[2]Institute Matériaux Microélectronique Nanosciences de Provence, UMR 6242 CNRS, Université Aix-Marseille, 13397 Marseille Cedex 20, France

*Correspondence should be addressed to: yaping.dan@sjtu.edu.cn

Section 1. Other forms of Ohmic contacts

In this section, We performed the 2D simulations using Silvaco on a silicon slab. The following models are included in the simulations: Auger recombination model, SRH recombination model, Universal Schottky tunneling model and Fermi-Dirac carrier statistic model. The generation rate is set uniformly at 2.48×10^{20} cm^{-3}. The mobility of electrons and holes are 708 cm^2/Vs and 236 cm^2/Vs, respectively. The lifetime of electrons and holes are both set at 1ns.

1) Ohmic contacts formed by tunneling through a Schottky junction

The device structure is shown in the panel (a) of Fig.S1. The work function of the metal is 4.8eV and the electron affinity of silicon is 4.17 eV. To facilitate Ohmic contacts by tunneling, the p-type silicon (20nm thick) in contact with the metal is highly doped. The energy band diamgram is shown in the panel (b). The Schottky barrier heigh is about 0.5 eV and the depletion region thickness is about 1-9 nm depending on the doping concentration. When the P$^+$ region is doped at 1×10^{19} cm^{-3}, the depletion region thickness is a little large (~9nm). The dark current is nonlinear shown as the red curve

in panel (c). When the doping concentration is increased to 3×10^{19} cm^{-3}, the depletion region is narrowed down ~2 nm shown in the closeup plot in panel (b). The dark current becomes linear shown as the black line in panel (c), although at very high voltage it becomes slightly nonlinear (inset in panel (c)). In this case, the photocurrent is nonlinear and saturates to a value lower than eGL as shown in the panel (d), meaning no photogain.
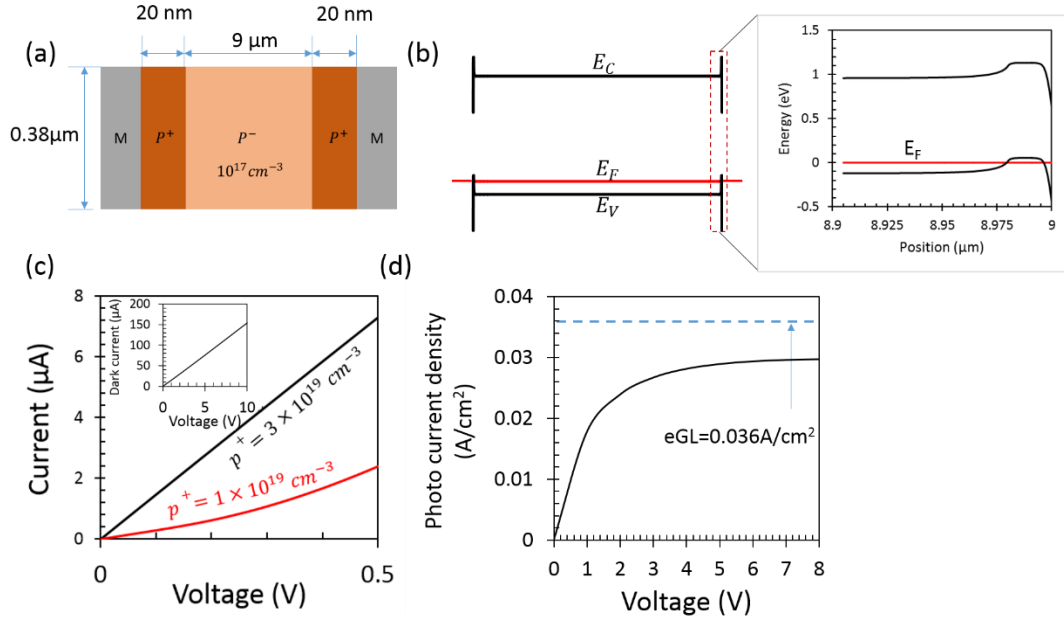

Fig.S1 Schematic, energy band diagram, dark current and photocurrent of a photoconductor in Ohmic contacts with metal by tunneling through a Schottky barrier.

2) Silicide Ohmic contacts

We assume that the silicon in contact with the metal is formed a silicide layer after the device is annealed at elavated temperature, as shown in Fig.S2 (a). The silicide is 10nm thick. Silicides are silicon and metal alloys which are semiconductors with a small bandgap. To mimic this case, we assume that the silicide has a bandgap of 0.38eV and the electron affinity larger than silicon, creating an energy band diamgram as shown in Fig. S2 (b). A closeup figure of the band diagram at Si-silicide interface is shown in the inset. Fig.2S (c) shows the dark current vs voltage which is linear. The photocurrent will saturate to a value less than eGL = 0.036 A/cm2 at high voltage bias, as shown in
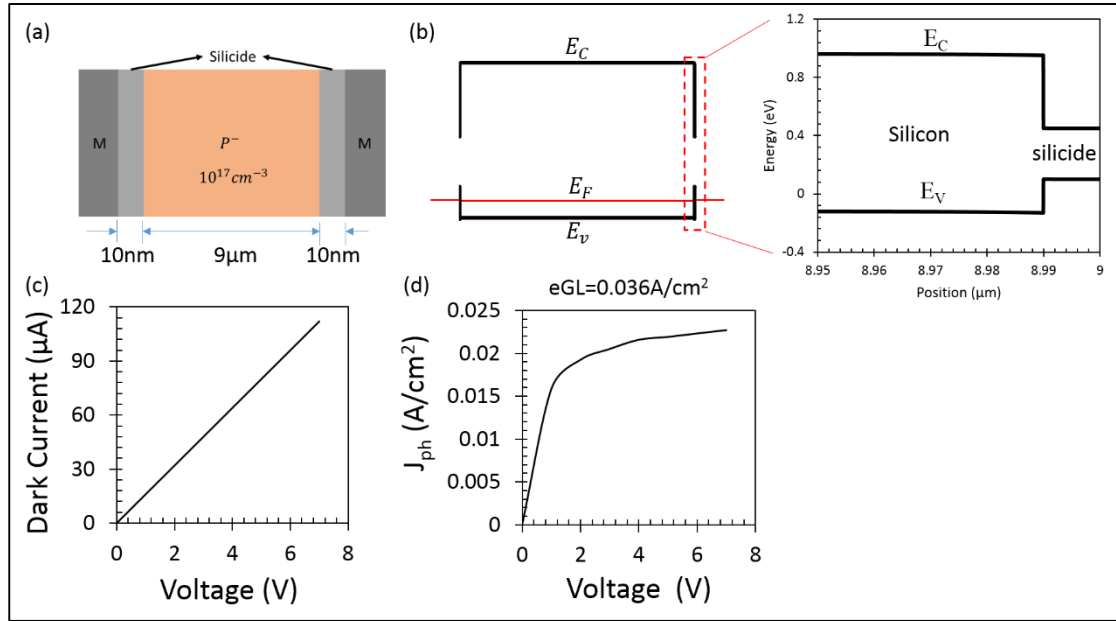
Fig.S2 (d).

Figure S2. Simulation results for a photoconductor in Ohmic contact with metal by forming silicides at the interface.

Section 2. Ambipolar transportation

The simulations were performed by using the Lumerical DEVICE software. The device under simulation is 50 μm long and 1 μm × 1 μm in cross-section. It has a uniform p type doping of 1×10^{17} cm^{-3}. The generation rate is a constant of 1×10^{22} cm^{-3}s^{-1}. Trap-assisted recombination, radiative recombination, surface recombination and auger recombination were excluded from the simulation. Velocity saturation effect is also excluded from the simulation. The mobility and lifetime is varied under different cases. Voltage bias is applied between anode and cathode.
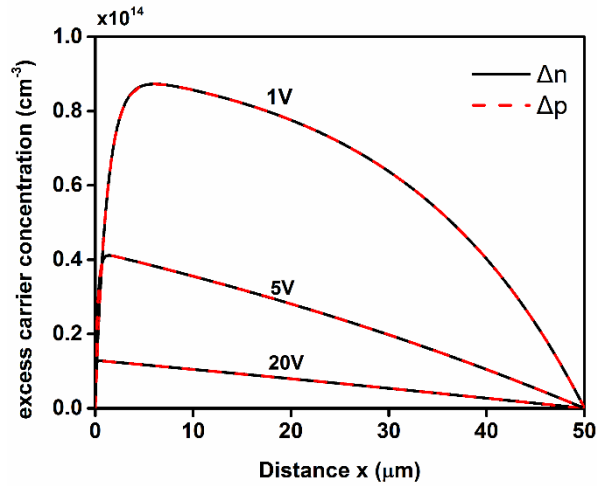
Fig. S3. Spatial distribution of photogenerated excess electrons and holes in a photoconductor under different voltage bias. The electron and hole mobility are 875 cm^2/Vs and 337 cm^2/Vs, respectively, the minority carrier lifetime is 10ns.

Device simulation shows that the spatial distributions of excess majority and minority carriers are always identical under different voltage bias, showing an ambipolar transport phenomenon.

Section 3. Surface States and Fixed Charges

The two dimensional simulations with surface states and fixed charge were performed using Silvaco Atlas software. The fixed charge in the simulations are uniform distributed at the surface, and the density distribution of acceptor-type and donor-type surface states are shown in Fig. S4. During the simulations, the peak of the surface states density varies from 5×10^9 to 4×10^{12} cm^{-2} eV^{-1} . The fixed charge density is selt at 0, 3×10^{11} and 7×10^{11} cm^{-2}. We assumed that the nanowire length L and thickness w are 9μm and 380nm, respectively. The p-type doping concentration is $1.05 \times 10^{17} cm^{-3}$. Apart from that, electron and hole life time are assumed as 200 ns and 100 ns respectively. The nanowire surfaces are covered with a layer of silicon oxide.
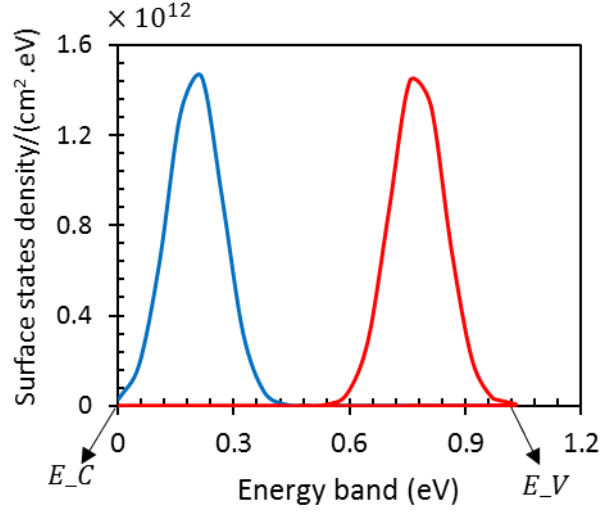
Fig. S4. Density distribution of acceptor-type and donor-type surface states in energy bandgap used in the simulations. Similar distribution patterns of surface states on Si/SiO$_2$ interface have been reported[1].

In the simulations, the hole and electron mobility are set as 236 cm^2/Vs and 708 cm^2/Vs, respectively, and the external voltage U is set as 1V. We can further obtain the transient time for minority carriers τ_t by

$$\tau_t = \frac{L}{\mu_n \left(\frac{U}{L}\right)}. \tag{S1}$$

The transient time τ_t can be calculated as 1.14× 10^{-9}s.

By setting the illumination source with wavelength of 460nm and light intensity of 10mW·cm^{-2}, an average photo generation rate g of 2.58× 10^{20} cm^{-3}s^{-1} shall be obtained in the simulation. The effective minority carrier life time $\tau_{n,eff}$ can be written as

$$\tau_{n,eff} = \overline{\Delta n}/g \tag{S2}$$

where $\overline{\Delta n}$ is the average excess electron concentration in the nanowire.

Photo gain G expressed by quantum efficiency shall be written as

$$G = \frac{\Delta J}{egL}, \tag{S3}$$

where ΔJ is the photo current density.

G' is defined as

$$G' = \overline{\Delta p} \Big/ \overline{\Delta n} \tag{S4}$$

where $\overline{\Delta p}$ and $\overline{\Delta n}$ is the average excess hole and electron concentration in the nanowire, respectively.
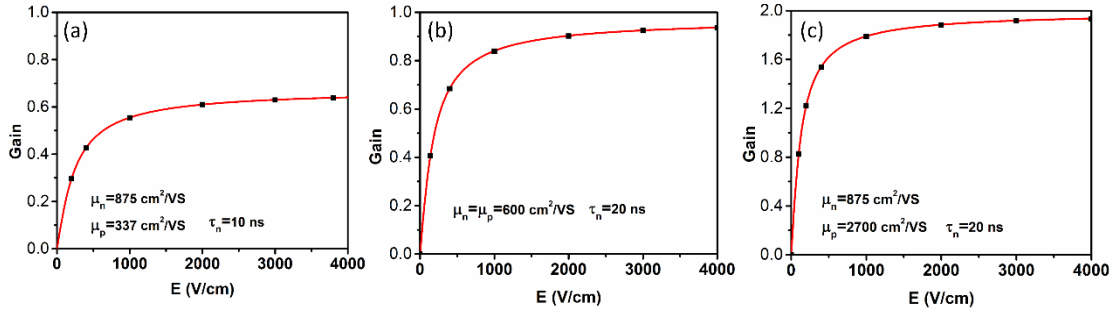
Section 4. Photo Gain

Fig. S5. Simulated photogain (red line) and calculated with eq. (S5) (black square dots).

The red line in Fig.S5 is taken from Fig.3 in the main text. The gain is calculated by divide the photocurrent density with eg_nL. The black square dots are calculated as following. The spatial distribution of photogenerated excess electrons $\Delta n(x)$ is obtained from DEVICE simulation, as shown in Figure 2 in the main text. The average excess carrier concentration

$$\overline{\Delta n} = \frac{\int_0^L \Delta n(x)dx}{L}$$

The effective minority carrier lifetime $\tau_{n,eff}$ can be written as $\tau_{n,eff} = \overline{\Delta n}/g$ where g is the carrier generation rate. When G' is equal to 1, the gain is then

calculated with the following equation:

$$G = \frac{\tau_{n,eff}}{L}(\mu_n + \mu_p)E \qquad \text{eq.(S5)}$$

References

[1] Seiffe J, Hofmann M, Rentsch J, Preu R. "Charge carrier trapping at passivated silicon surfaces". Journal of Applied Physics 2011; 109(6): 064505.